NASA TECHNICAL MEMORANDUM

NASA TM X-3159

NASA TM X-3159

INFLUENCE OF CONFIGURATION DETAILS ON THE SUBSONIC CHARACTERISTICS OF A SPACE SHUTTLE ORBITER DESIGN

John P. Decker and W. Pelham Phillips

Langley Research Center

Hampton, Va. 23665

NATIONAL AERONAUTICS AND SPACE ADMINISTRATION • WASHINGTON, D. C. • DECEMBER 1974

1. Report No.	2. Government Accession No.	3. Recipient's Catalog No.
NASA TM X-3159		

4. Title and Subtitle	5. Report Date
INFLUENCE OF CONFIGURATION DETAILS ON THE SUBSONIC CHARACTERISTICS OF A SPACE SHUTTLE ORBITER DESIGN	December 1974
	6. Performing Organization Code
7. Author(s)	8. Performing Organization Report No.
John P. Decker and W. Pelham Phillips	L-9722
	10. Work Unit No.
9. Performing Organization Name and Address	502-37-01-01
NASA Langley Research Center Hampton, Va. 23665	11. Contract or Grant No.
	13. Type of Report and Period Covered
12. Sponsoring Agency Name and Address	Technical Memorandum
National Aeronautics and Space Administration Washington, D.C. 20546	14. Sponsoring Agency Code

15. Supplementary Notes

16. Abstract

An investigation was conducted in the Langley low-turbulence pressure tunnel of a model of a space shuttle orbiter design in order to determine the influence of minor configuration geometric details on the aerodynamic characteristics at subsonic speeds. A plane wing was tested with a small planform fillet; a twisted wing was tested with both a small and a large planform fillet. Tailored attitude-control propulsion-system wing-tip and body pods, trisegmented elevons, and canopy effects were also investigated. The tests were conducted at angles of attack from -3° to 24° for sideslip angles of 0° and 6° and at a Mach number of 0.25.

17. Key Words (Suggested by Author(s))	18. Distribution Statement
Space shuttle Aerodynamics	Unclassified – Unlimited STAR Category 31

19. Security Classif. (of this report)	20. Security Classif. (of this page)	21. No. of Pages	22. Price*
Unclassified	Unclassified	27	$3.75

*For sale by the National Technical Information Service, Springfield, Virginia 22151

INFLUENCE OF CONFIGURATION DETAILS ON THE SUBSONIC CHARACTERISTICS OF A SPACE SHUTTLE ORBITER DESIGN

By John P. Decker and W. Pelham Phillips
Langley Research Center

SUMMARY

An investigation was conducted in the Langley low-turbulence pressure tunnel of a model of a space shuttle orbiter design in order to determine the influence of minor configuration geometric details on the aerodynamic characteristics at subsonic speeds. A plane wing was tested with a small planform fillet; a twisted wing was tested with both a small and a large planform fillet. Tailored attitude-control propulsion-system wing-tip and body pods, trisegmented elevons, and canopy effects were also investigated. The tests were conducted at angles of attack from -3° to 24° for sideslip angles of 0° and 6° and at a Mach number of 0.25.

The configuration with a plane wing and a small wing-planform fillet had a small region of pitch-up at the higher angles of attack. The combination of linear wing twist (4.5° washout) and a larger wing-planform fillet linearized both the pitch and the lift curves at angles of attack up to about 20° and produced increases in trimmed lift at these higher angles of attack. This configuration had a maximum trimmed lift-drag ratio of 7.0.

The addition of large, tailored wing-tip pods, sized to house the complete attitude-control propulsion-system package, or the addition of small, tailored wing-tip pods in combination with tailored body pods, together housing the entire attitude-control propulsion-system package, did not penalize the performance of the vehicle significantly. Using trisegmented elevons having spanwise variations in the deflection angle, with the plane wing and with the small planform fillet, increased the trimmed maximum lift-drag ratio by about 5 percent over the value obtained by using full-span elevons. The removal of the canopy decreased the drag and increased the maximum lift-drag ratio by about 5 percent.

Limited lateral-directional stability data were obtained for the configuration with the twisted wing and the small planform fillet. These data indicated that the configuration had a positive effective dihedral and a positive static-directional stability at all test angles of attack.

INTRODUCTION

The National Aeronautics and Space Administration is currently proceeding with the development of a space shuttle system. Prior to the selection of the space shuttle prime contractor, Rockwell International, the NASA conducted several in-house design studies in order to produce candidate space shuttle orbiter configurations. One of the orbiter design studies (ref. 1) employed an analytical design synthesis tool to define an orbiter wing configuration which would achieve low landing speeds while maintaining compatibility with high angle-of-attack hypersonic trim requirements.

Subsequent experimental verification studies at low speeds of the analytically designed orbiter configuration (also reported in ref. 1) indicated a pitch down at high angles of attack and associated losses in lift relative to the analytically predicted values. The addition of a planform fillet provided the desired lift and pitch linearization at high angles of attack. Because of the influence of the planform fillet, the present study was initiated in order to determine some effects of the planform-fillet size as well as the effects of wing twist in combination with the planform fillets.

The limited aerodynamic data from reference 2 indicated significant degradations in trimmed lift-drag ratios associated with the addition of unfaired wing-tip-mounted pods designed to house the attitude control propulsion system (ACPS). The total ACPS includes the roll, the pitch, and the yaw jets plus the propellant tankage. In reference 1, the data were obtained for some small, tailored wing-tip-mounted pods sized to house only the roll-control jets and the associated tankage. It was found that these pods produced only a small decrement in the trimmed lift-drag ratio. In the present investigation, the work of reference 1 has been extended in order to provide data for tailored pods of a sufficient size to house the total ACPS for an operational orbiter having mass properties similar to those of the configuration of reference 1. Results were also obtained which determine the effects of the trisegmented elevons and of the canopy.

SYMBOLS

The data of the present investigation are referred to the body-axis system with the exception of the lift and drag coefficients, which are referred to the stability-axis system. All coefficients are based on the geometry of the basic wing planform. The data for the configuration with the small planform fillet were reduced about a center of gravity located at 65.0 percent of the body length along the model reference line. The data for the configuration with the large planform fillet were reduced about a center of gravity located at 63.8 percent of the body length along the model reference line. (See fig. 1.) Values are presented in the International System of Units (SI) and U.S. Customary Units. Measurements and calculations were made in U.S. Customary Units.

b	wing span, 51.69 cm (20.35 in.)
C_D	drag coefficient, $\frac{\text{Drag}}{q_\infty S}$
C_L	lift coefficient, $\frac{\text{Lift}}{q_\infty S}$
C_l	rolling-moment coefficient, $\frac{\text{Rolling moment}}{q_\infty Sb}$
C_{l_β}	rolling-moment parameter, $\frac{\Delta C_l}{\Delta\beta}$, $\beta = 0^\circ, 6^\circ$
C_m	pitching-moment coefficient, $\frac{\text{Pitching moment}}{q_\infty S\bar{c}}$
C_n	yawing-moment coefficient, $\frac{\text{Yawing moment}}{q_\infty Sb}$
C_{n_β}	yawing-moment parameter, $\frac{\Delta C_n}{\Delta\beta}$, $\beta = 0^\circ, 6^\circ$
C_Y	side-force coefficient, $\frac{\text{Side force}}{q_\infty S}$
C_{Y_β}	side-force parameter, $\frac{\Delta C_Y}{\Delta\beta}$, $\beta = 0^\circ, 6^\circ$
$\bar{c}$	wing mean aerodynamic chord, 25.55 cm (10.06 in.)
L/D	lift-drag ratio
l	length of fuselage, cm (in.)
M	free-stream Mach number
q_∞	free-stream dynamic pressure
R	Reynolds number based on l
S	reference wing area, 0.110 m^2 (1.19 ft^2)
α	angle of attack, deg
β	angle of sideslip, deg
$\delta_{e_1}, \delta_{e_2}, \delta_{e_3}$	inboard-to-outboard deflections of elevon segments, trailing edge down is positive

Subscript:

max	maximum

Abbreviations:

ACPS	attitude control propulsion system
B	body
F_1	small planform fillet
F_2	large planform fillet
P_2	tailored small wing-tip ACPS pods
P_3	tailored large wing-tip ACPS pods
P_B	tailored body ACPS pods
V	vertical tail
W_P	plane wing
W_T	twisted wing

APPARATUS AND TESTS

Model

Details of the 0.01875-scale model are shown in figure 1 and the pertinent geometric characteristics are given in table I. The basic model without planform fillets was the same as the subsonic model of reference 1, except that the wing of the present model was moved aft 0.0146ℓ in order to insure subsonically stable static margins with the small fillet (F_1) installed for all the anticipated payload conditions indicated in reference 1. The basic wing planform (without planform fillet) had the leading edge swept 46.8°, the trailing edge swept -11.2°, and trisegmented elevons. (See fig. 1(a).) The basic wing airfoil sections varied from an NACA 0008-64 section at the exposed root chord to an NACA 0012-64 section at the tip chord.

Two basic wings identical in projected planform were tested: a plane (untwisted) wing (W_P) with a 1.5° incidence, and a twisted wing (W_T) with the same incidence at the exposed root chord and 4.5° washout. The plane wing was tested with a small 60° swept-planform fillet; the twisted wing was tested with both a small and a large 60° swept-planform fillet. The large fillet (F_2) was the same as the fillet tested in reference 1. The F_2 fillet increased the exposed wing area by about 8.5 percent whereas the F_1 fillet provided an exposed-area increase of about 5.5 percent. The planform-fillet airfoil sections had a leading-edge radius of about 0.20 cm (0.078 in.) and were smooth fairings from the leading edge to the 40-percent chord stations of the basic wing planform.

The basic wing apex was located at 0.4275ℓ (see fig. 1(a)) and the moment reference center for the configuration with F_1 was located at 0.650ℓ. In order to insure similar static-margin levels for comparative purposes, the data for F_2 were referenced to a moment center located at 0.638ℓ.

Two concepts of tailored ACPS pods (fig. 1(c)) were tested. Small wing-tip-mounted pods (P_2) were tested in combination with large body-mounted pods (P_B). The P_2 pods were identical to the pods of reference 1 and were sized to contain the roll-control ACPS. The P_B pods were sized to house the remainder of the ACPS (that is, pitch and yaw). Large wing-tip-mounted pods P_3, sized to contain the total ACPS, were also tested).

The model vertical-tail geometry is described in table I. The tail had an aspect ratio of 1.95 and a leading-edge sweep angle of 45°. The airfoil section was an NACA 0012-64.

Tunnel

The tests were conducted in the Langley low-turbulence pressure tunnel which is a variable-pressure, single-return facility with a closed test section, 0.914 m (3.0 ft) wide and 2.29 m (7.5 ft) high. The tunnel is a low-subsonic Mach number facility ($M \leq 0.4$) with the capability of Reynolds numbers to 49.2×10^6 per meter (15.0×10^6 per foot).

Test Conditions

The investigation was conducted at a Mach number of about 0.25 and at Reynolds numbers based on the fuselage length from about 8.0×10^6 to 23.7×10^6. The test angle of attack varied from about -3° to 24° at 0° and 6° sideslip angles.

Measurements and Corrections

An internally mounted, six-component strain-gage balance was used to measure the aerodynamic forces and moments acting on the model. No base pressure corrections

were applied to the data. Corrections have been applied to the angles of attack and the sideslip in order to account for the sting deflections produced by aerodynamic loads on the model. The longitudinal aerodynamic coefficients and angles of attack have been corrected for blockage and lift interference in accordance with the techniques outlined in references 3 and 4. No corrections have been applied for tunnel-flow misalinement or for wall interference on the lateral-directional aerodynamic coefficients since previous tests on models of similar size have indicated that the flow-misalinement angle is negligible. The effect of the wall interference on the lateral-directional aerodynamic coefficients is a direct function of the projected lateral area and the magnitude of the side-force coefficient. This correction was also found to be negligible.

RESULTS AND DISCUSSION

Longitudinal Aerodynamic Characteristics

The basic longitudinal aerodynamic characteristics are shown in figures 2 to 7. The trim characteristics are summarized in figure 8.

Effect of Reynolds number.- Increasing the Reynolds number, based on fuselage length, from 8.0×10^6 to 23.7×10^6 indicated only minor effects at Reynolds numbers greater than 15.8×10^6 on the longitudinal aerodynamic characteristics of the configuration with the twisted wing and small planform fillet (fig. 2). This is in agreement with the results found in reference 1. Accordingly, most of the tests were conducted at a Reynolds number of 15.8×10^6.

Effect of wing twist and planform fillet size.- Figure 3 shows that the configuration with the untwisted wing and the small planform fillet had pitch-up at the higher lift coefficients. The incorporation of a linear wing twist (4.5° washout) tended to alleviate the severity of the pitch-up characteristics of the configuration. (See fig. 4.) The combination of the linear wing twist and the large planform fillet (fig. 5) linearized the pitch curves at the higher angles. In addition, the larger planform fillet linearized the lift curve to angles of attack of about 20° and produced increases in the trimmed C_L at the higher angles of attack. (See fig. 8.) Figure 8 also shows that the linear wing twist had no effect on the trimmed $(L/D)_{max}$; however, the larger planform fillet decreased the trimmed $(L/D)_{max}$ from about 7.4 to 7.0.

Effect of segmented elevons.- The effects of the trisegmented elevons on the plane-wing small-fillet configuration are shown in figure 3 and summarized in figure 8. Spanwise variations in the elevon deflection angle increased the trimmed lift-drag ratio about 5 percent over the value obtained by using the full-span elevons, with little change in the trimmed lift coefficient. (See fig. 8.) This result is similar to the result obtained in

reference 1, with the exception that the current data is for a wing with a planform fillet, whereas the data of reference 1 did not have a planform fillet.

Effect of ACPS pods.- The addition of orbiter wing-tip-mounted ACPS pods and body-mounted ACPS pods has produced significant degradations in the subsonic L/D in previous applications. (See ref. 2.) The results from reference 2 indicated a decrement in the $(L/D)_{max}$ of 1.2 which would result in an approach glide-slope angle increase somewhat greater than 1^{o}. In reference 1, the data were obtained from small, tailored, roll-control wing ACPS pods. It was found that these pods produced a decrement of only 0.1 in the $(L/D)_{max}$ while increasing the lift of the configuration due to the end-plating effect. In the present investigation, the work of reference 1 has been extended to provide data for tailored pods of sufficient size to house the volume estimated to be necessary for the total ACPS. Figure 6 presents the results obtained from tests of a combination of the small wing-tip pods of reference 1 and tailored body-mounted ACPS pods (P_2P_B) and from larger wing-tip-mounted pods (P_3). For the two pod combinations tested, the largest $(L/D)_{max}$ decrement was less than 0.2. This decrement is attributed to the tailoring of the pods which minimized the form-drag increase and the end-plating effect.

Effect of canopy.- Figure 7 shows that the removal of the canopy produced no effect on the pitch and lift characteristics of the configuration. However, the removal of the canopy decreased the drag and increased the $(L/D)_{max}$ of the configuration by about 5 percent.

Lateral-Directional Aerodynamic Characteristics

Figure 9 presents some lateral-directional aerodynamic characteristics obtained in this investigation for the twisted wing with the small planform fillet. Data are shown with and without the vertical tail on the configuration and indicate that the vertical tail contributed significantly to the production of favorable lateral-directional aerodynamic characteristics. The complete configuration had a positive effective dihedral $\left(-C_{l_\beta}\right)$ and a positive directional stability $\left(+C_{n_\beta}\right)$ at all test angles of attack. At an angle of attack of about 8^{o}, there is a destabilizing effect on C_{l_β} and C_{n_β}. As was indicated in reference 2, this effect is caused by a vortex from the wing-body junction sweeping rearward along the body, creating a negative pressure gradient on the windward side aft of the center of gravity; destabilizing moments result.

CONCLUDING REMARKS

An investigation was conducted in the Langley low-turbulence pressure tunnel of a model of a space shuttle orbiter design in order to determine the influence of minor configuration geometric details on the aerodynamic characteristics of the configuration at

subsonic speeds. A plane wing was tested with a small planform fillet; a twisted wing was tested with both a small and a large planform fillet. Tailored attitude-control propulsion-system wing-tip and body pods, trisegmented elevons, and canopy effects were also investigated. The tests were conducted at angles of attack from -3° to 24° for sideslip angles of 0° and 6° and at a Mach number of 0.25. The investigation results indicated the following:

1. Increasing the Reynolds number, based on the fuselage length, from 8.0×10^6 to 23.7×10^6 had only minor effects on the longitudinal aerodynamic characteristics.

2. The configuration with a plane wing and small wing-planform fillet had a small region of pitch-up at the higher angles of attack. The combination of linear wing twist (4.5° washout) and a larger wing-planform fillet linearized both the pitch and lift curves at angles of attack up to about 20° and produced increases in trimmed lift at these higher angles of attack. This configuration, with the linear wing twist and large planform fillet, had a maximum trimmed lift-drag ratio of 7.0.

3. The addition of large, tailored wing-tip pods (sized to house the entire attitude-control propulsion-system package) or the addition of small tailored wing-tip pods tested in combination with tailored body pods (sized to house the entire attitude-control propulsion-system package) did not penalize the performance of the vehicle significantly.

4. The limited lateral-directional stability data that were obtained for the configuration with the twisted wing and small planform fillet indicate that the configuration had positive effective dihedral and positive static-directional stability at all test angles of attack.

5. Using trisegmented elevons having spanwise variations in the deflection angle with the plane wing and with the small planform fillet increased the maximum trimmed lift-drag ratio 5 percent over the value obtained by using full-span elevons.

6. The removal of the canopy decreased the drag and increased the maximum lift-drag ratio by about 5 percent.

Langley Research Center,
National Aeronautics and Space Administration,
Hampton, Va., November 26, 1974.

REFERENCES

1. Phillips, W. Pelham; Decker, John P.; Rau Timothy R.; and Glatt, C. R.: Computer-Aided Space Shuttle Orbiter Wing Design Study. NASA TN D-7478, 1974.

2. Freeman, Delma C., Jr.; and Ellison, James C.: Aerodynamic Studies of Delta-Wing Shuttle Orbiters. Pt. I – Low Speed. Vol. III of Space Shuttle Aerothermodynamics Technology Conference, NASA TM X-2508, 1972, pp. 785-801.

3. Herriot, John G.: Blockage Corrections for Three-Dimensional-Flow Closed Throat Wind Tunnels, With Consideration of the Effects of Compressibility. NACA Rep. 995, 1950.

4. Garner, H. C.: Lift Interference on Three-Dimensional Wings. Subsonic Wind Tunnel Wall Corrections, H. C. Garner, ed., AGARDograph 109, Oct. 1966, pp. 75-217.

TABLE I.- GEOMETRIC CHARACTERISTICS OF MODEL

Body:	
Length, cm (in.)	62.63 (24.656)
Base area, m^2 (ft^2)	0.009 (0.10)
Wetted area, m^2 (ft^2)	0.206 (2.22)
Basic wing:	
Area, total, m^2 (ft^2)	0.110 (1.19)
Span, cm (in.)	51.69 (20.35)
Aspect ratio, theoretical	2.42
Chord, center-line root, cm (in.)	37.72 (14.85)
Tip chord, cm (in.)	5.08 (2.00)
Mean aerodynamic chord, cm (in.)	25.55 (10.06)
Leading-edge sweep angle, deg	46.8
Trailing-edge sweep angle, deg	-11.2
Dihedral angle, deg	7.0
Incidence, exposed root chord, deg	
Plane wing	1.5
Twisted wing	1.5
Incidence, tip chord, deg	
Plane wing	1.5
Twisted wing	-3.0
Taper ratio	0.135
Airfoil section, exposed root	NACA 0008-64
Airfoil section, tip chord	NACA 0012-64
Elevons:	
Hinge line sweep angle, deg	0
Area, total, m^2 (ft^2)	0.022 (0.239)
Area, each elevon, m^2 (ft^2)	0.004 (0.040)
Planform fillets:	
Area, exposed, m^2 (ft^2)	
Small planform fillet, F_1	0.0067 (0.0725)
Large planform fillet, F_2	0.0041 (0.0439)
Leading-edge sweep angle, deg	
Small planform fillet, F_1	60
Large planform fillet, F_2	60
Vertical tail:	
Area, m^2 (ft^2)	0.016 (0.170)
Airfoil section	NACA 0012-64
Leading-edge sweep angle, deg	45
Span, equivalent, cm (in.)	17.58 (6.92)
Aspect ratio	1.95
Taper ratio	0.314
Root chord, cm (in.)	13.72 (5.40)
Tip chord, cm (in.)	4.29 (1.69)

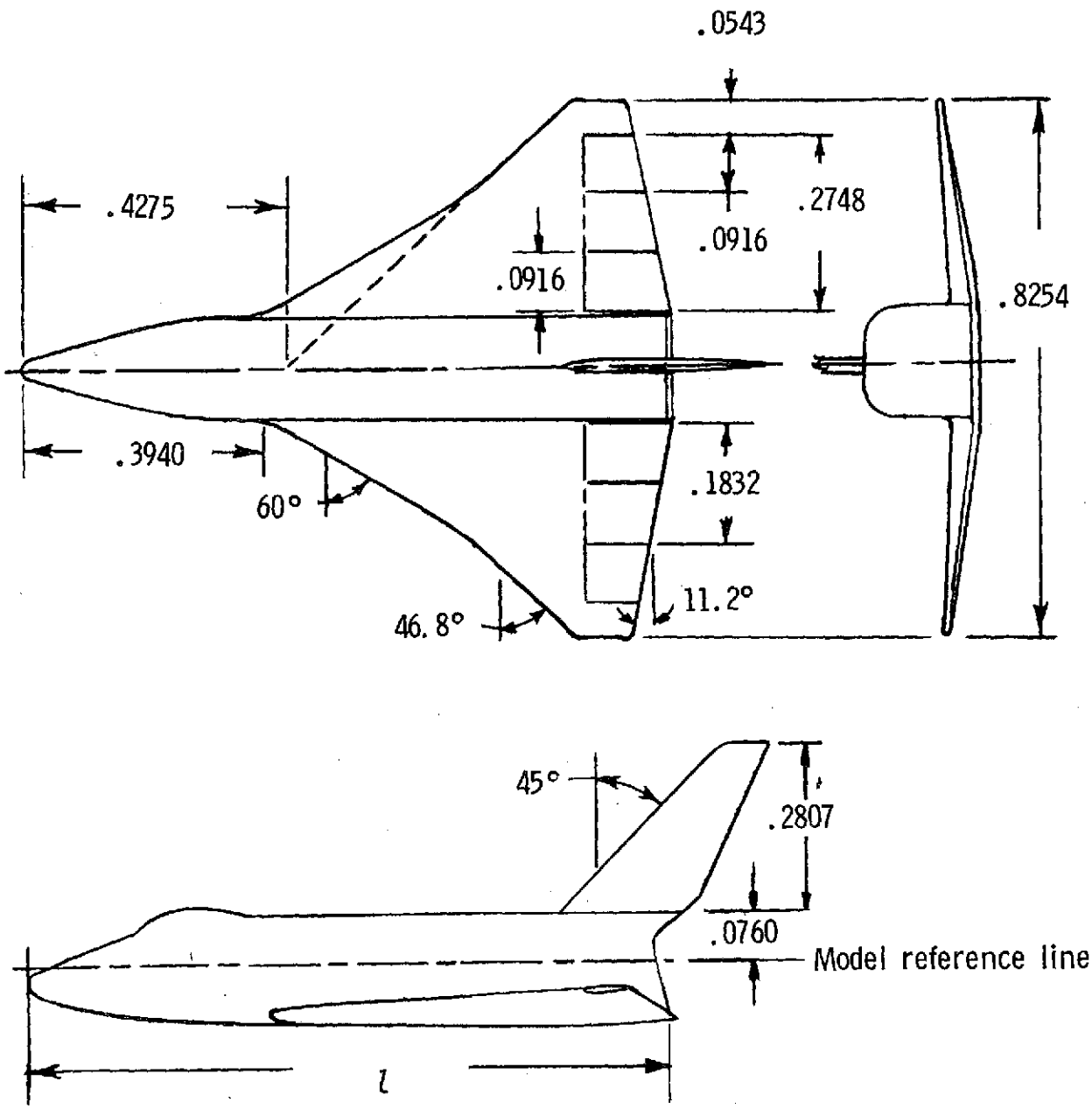

(a) 0.01875 model BW_TVF_1.

Figure 1.- Model schematics. All dimensions are normalized by the fuselage length (ℓ = 62.63 cm (24.656 in.)).

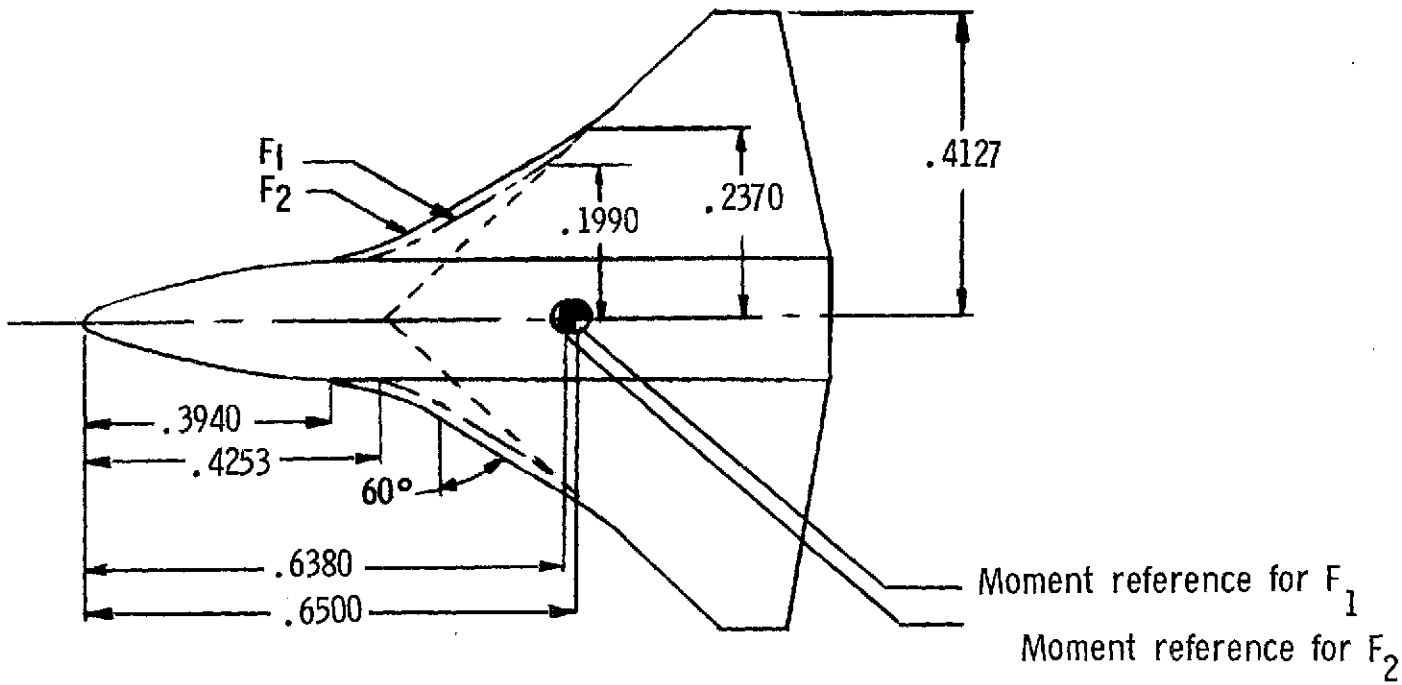

(b) Wing planform fillets.

Figure 1.- Continued.

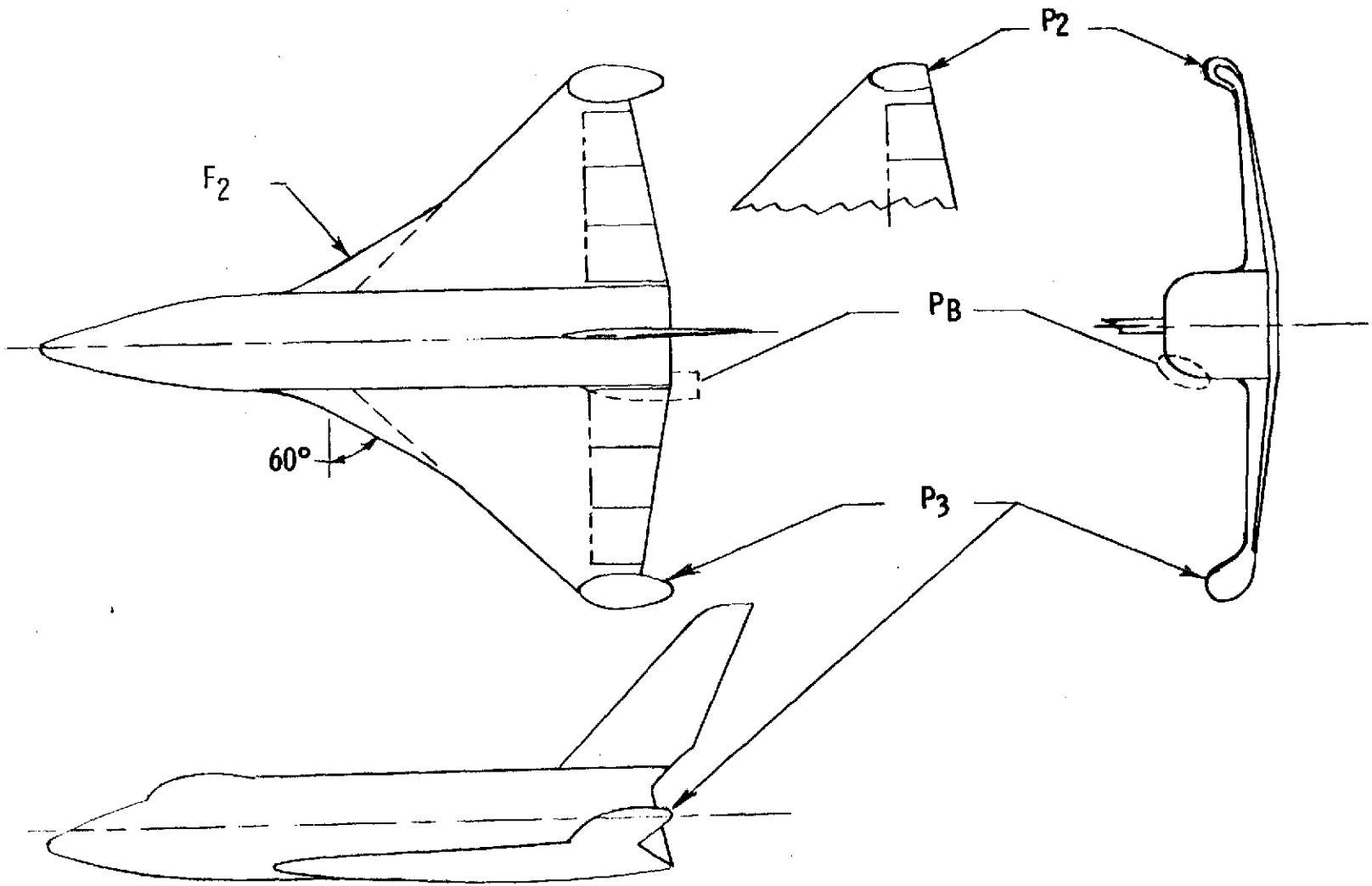

(c) ACPS pod details.

Figure 1.- Concluded.

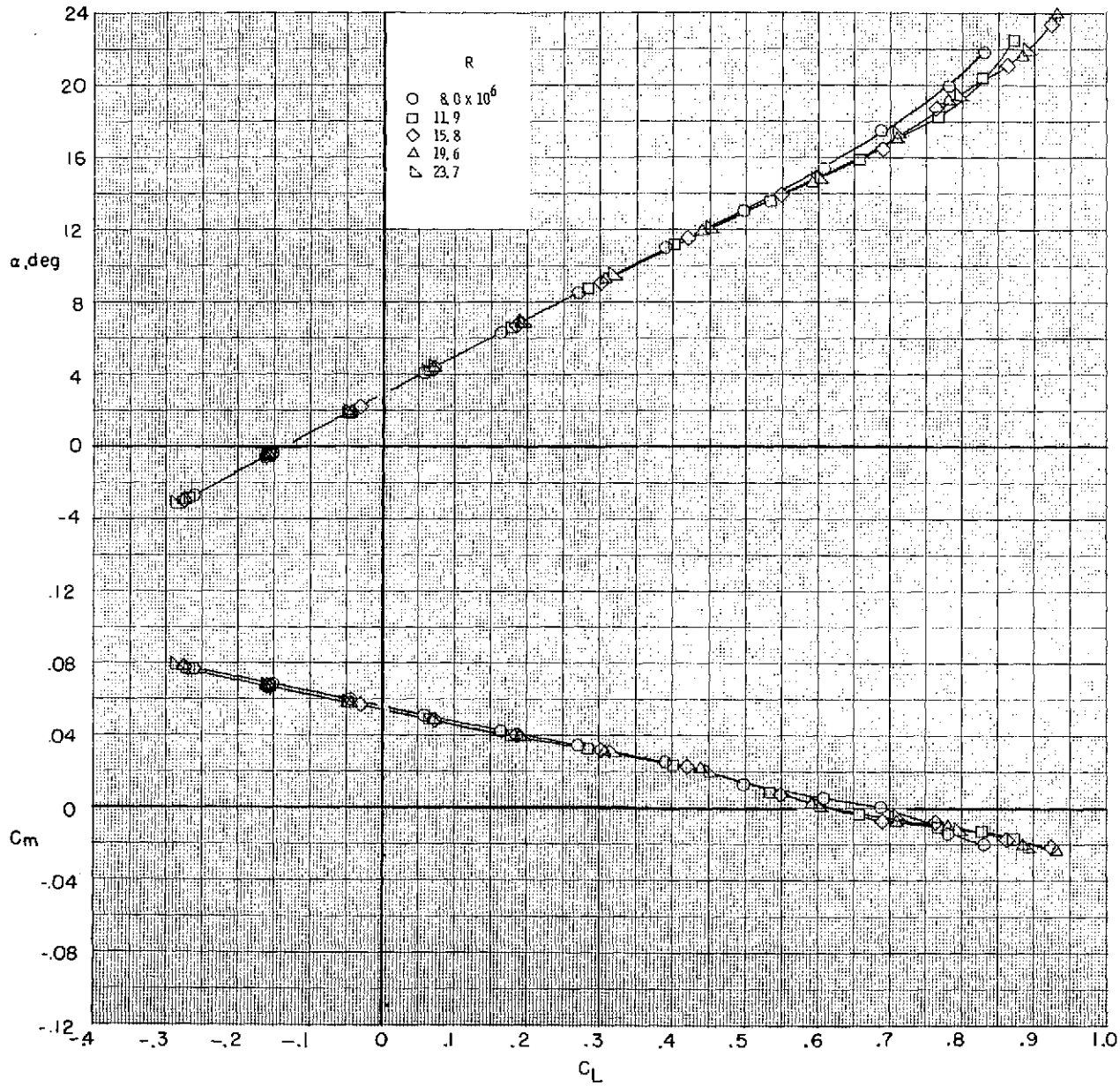

Figure 2.- Effect of Reynolds number on the longitudinal aerodynamic characteristics of $BW_TVF_1P_B$. $\delta_{e_1} = -10^o$; $\delta_{e_2} = -5^o$; $\delta_{e_3} = -5^o$.

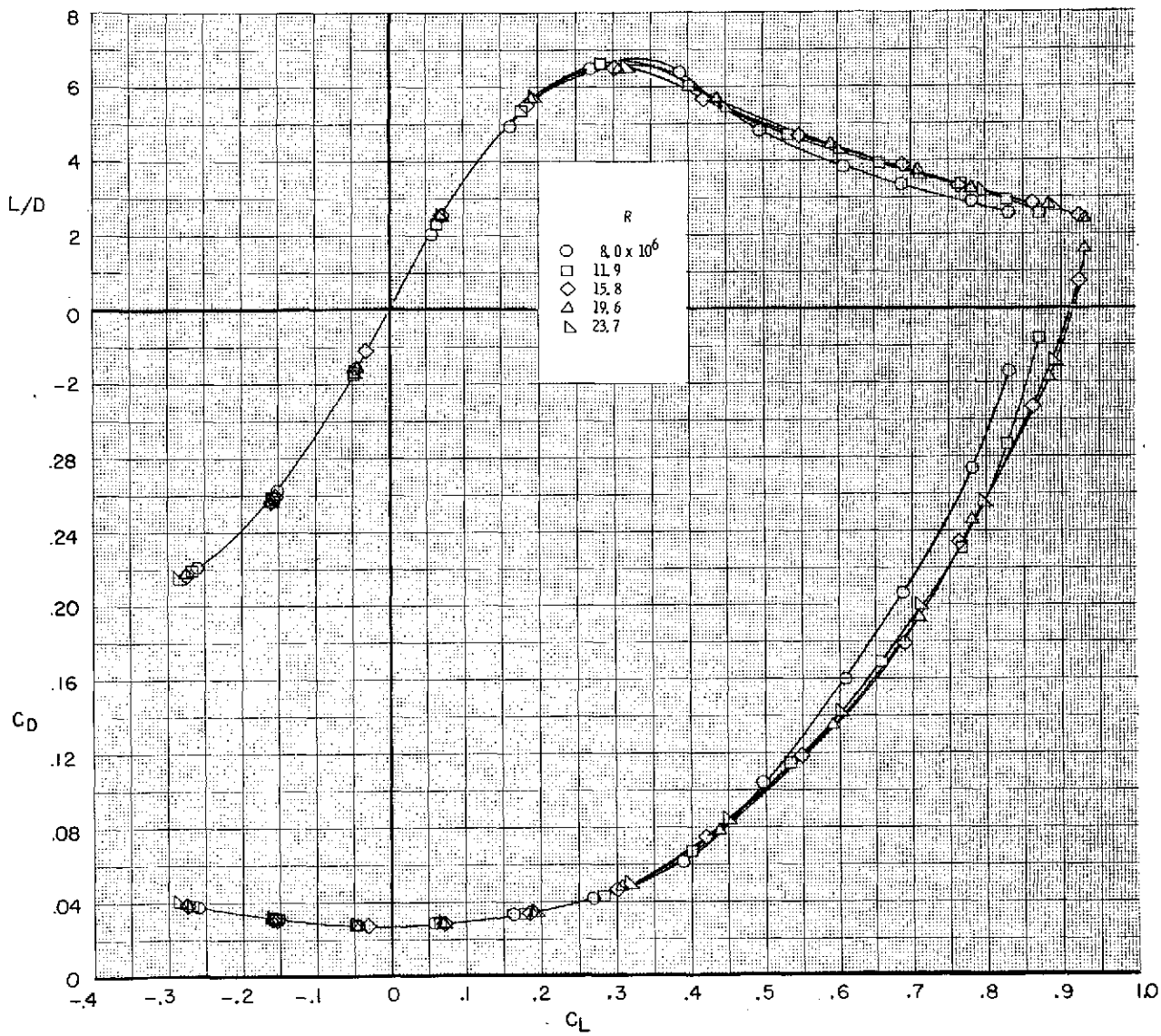

Figure 2.- Concluded.

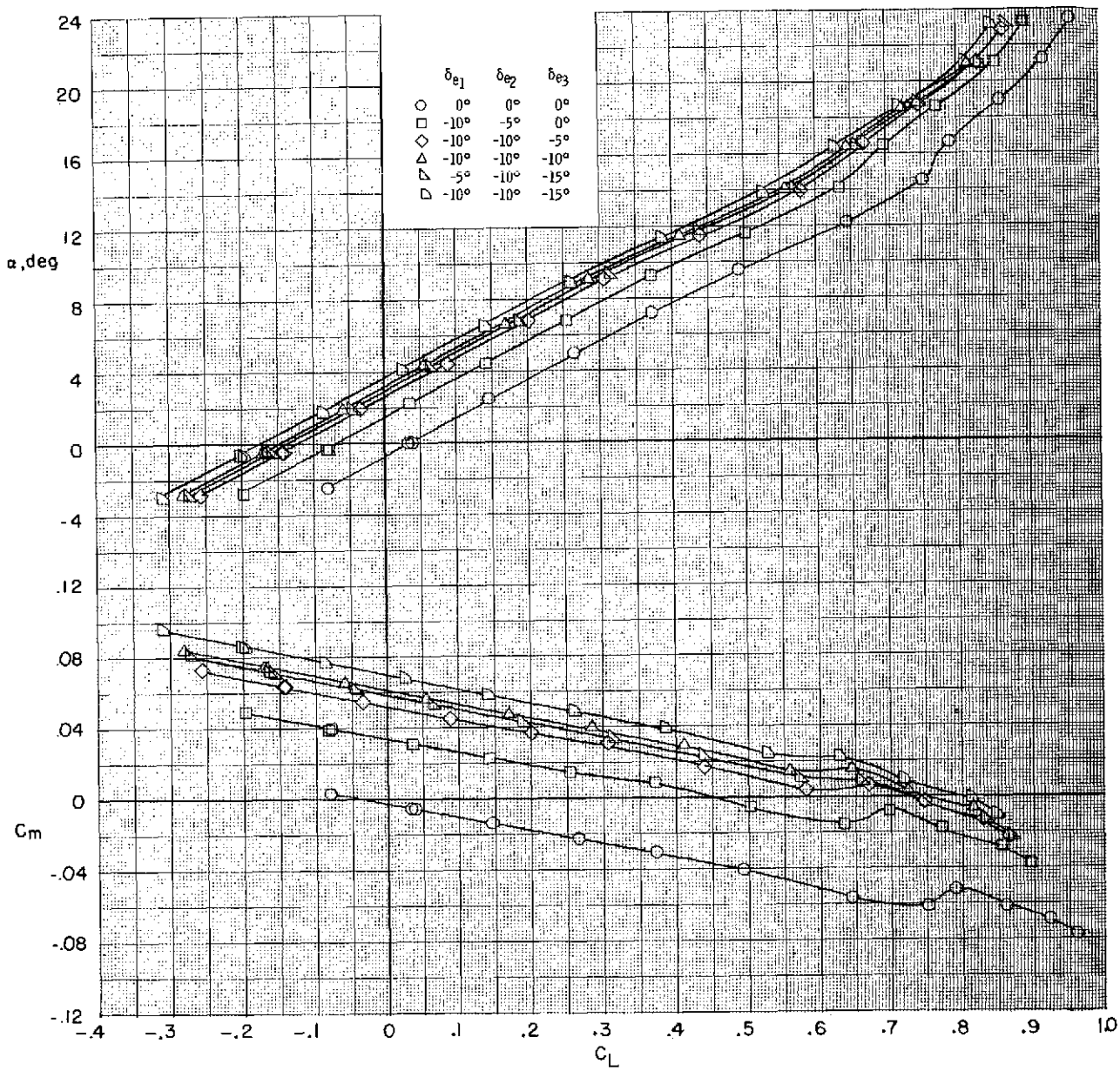

Figure 3.- Effect of elevon deflection on the longitudinal aerodynamic characteristics of BW_pVF_1. $R = 15.8 \times 10^6$.

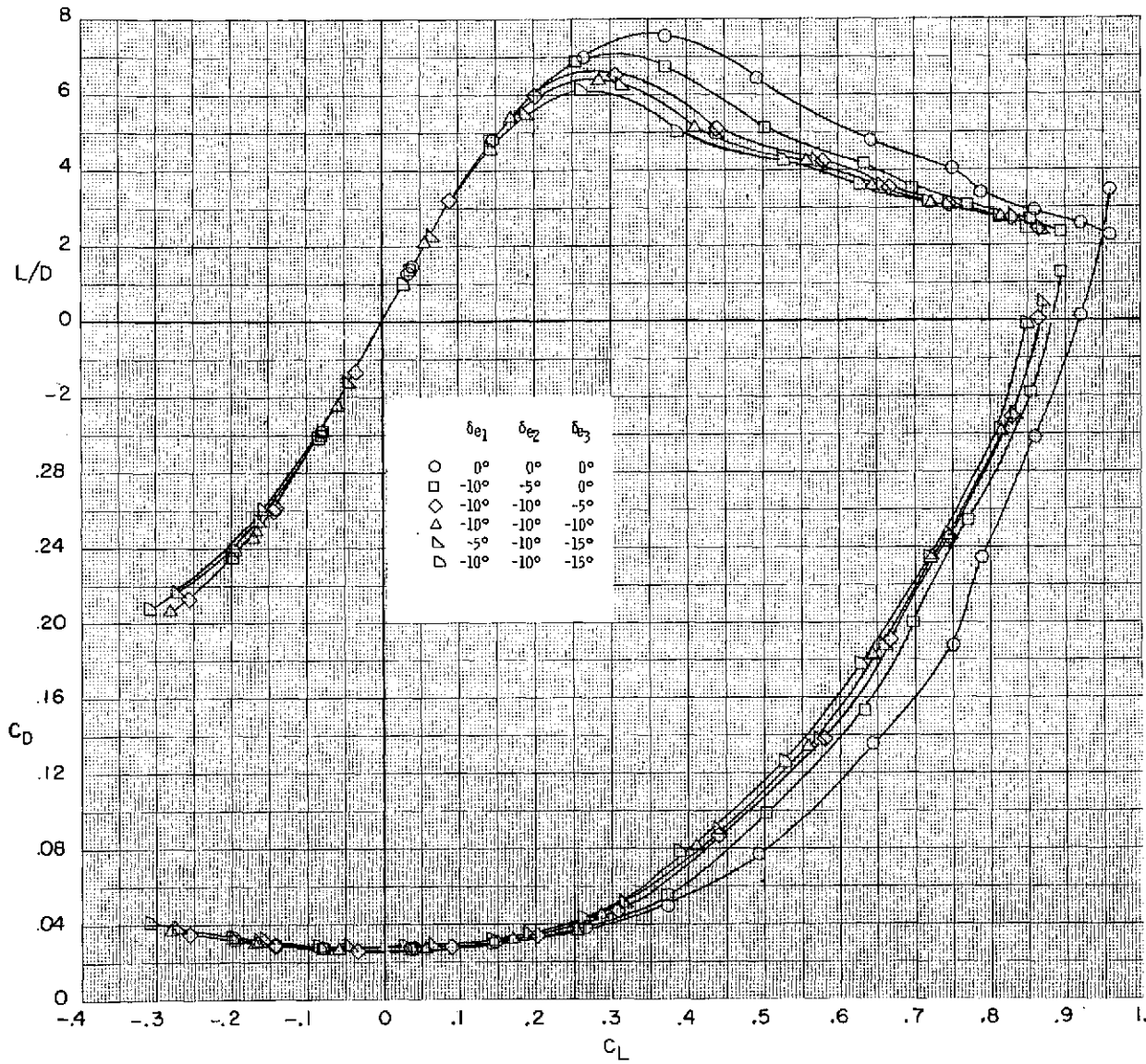

Figure 3.- Concluded.

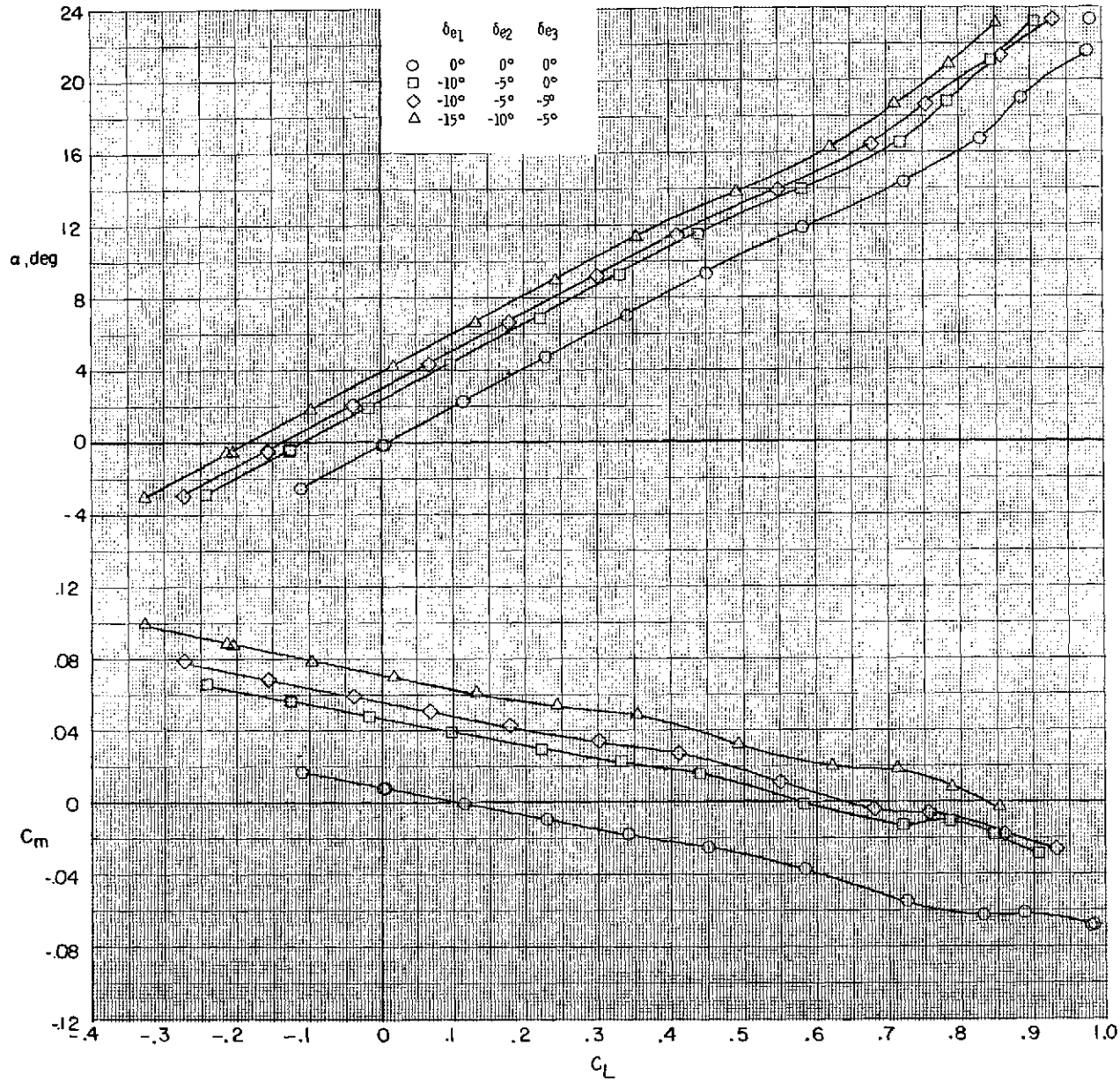

Figure 4.- Effect of elevon deflection on the longitudinal aerodynamic characteristics of BW_TVF_1. $R \doteq 15.8 \times 10^6$.

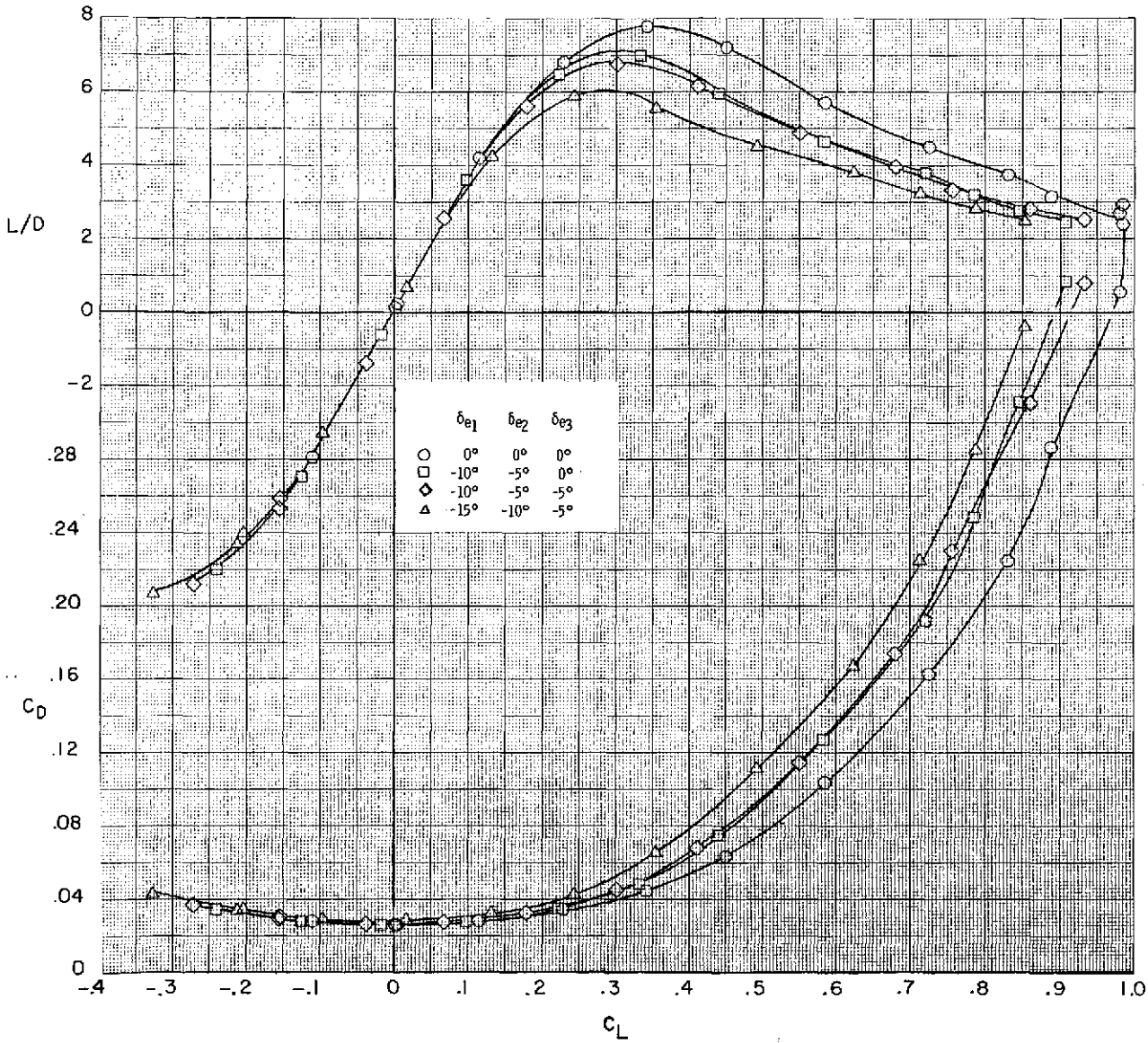

Figure 4.- Concluded.

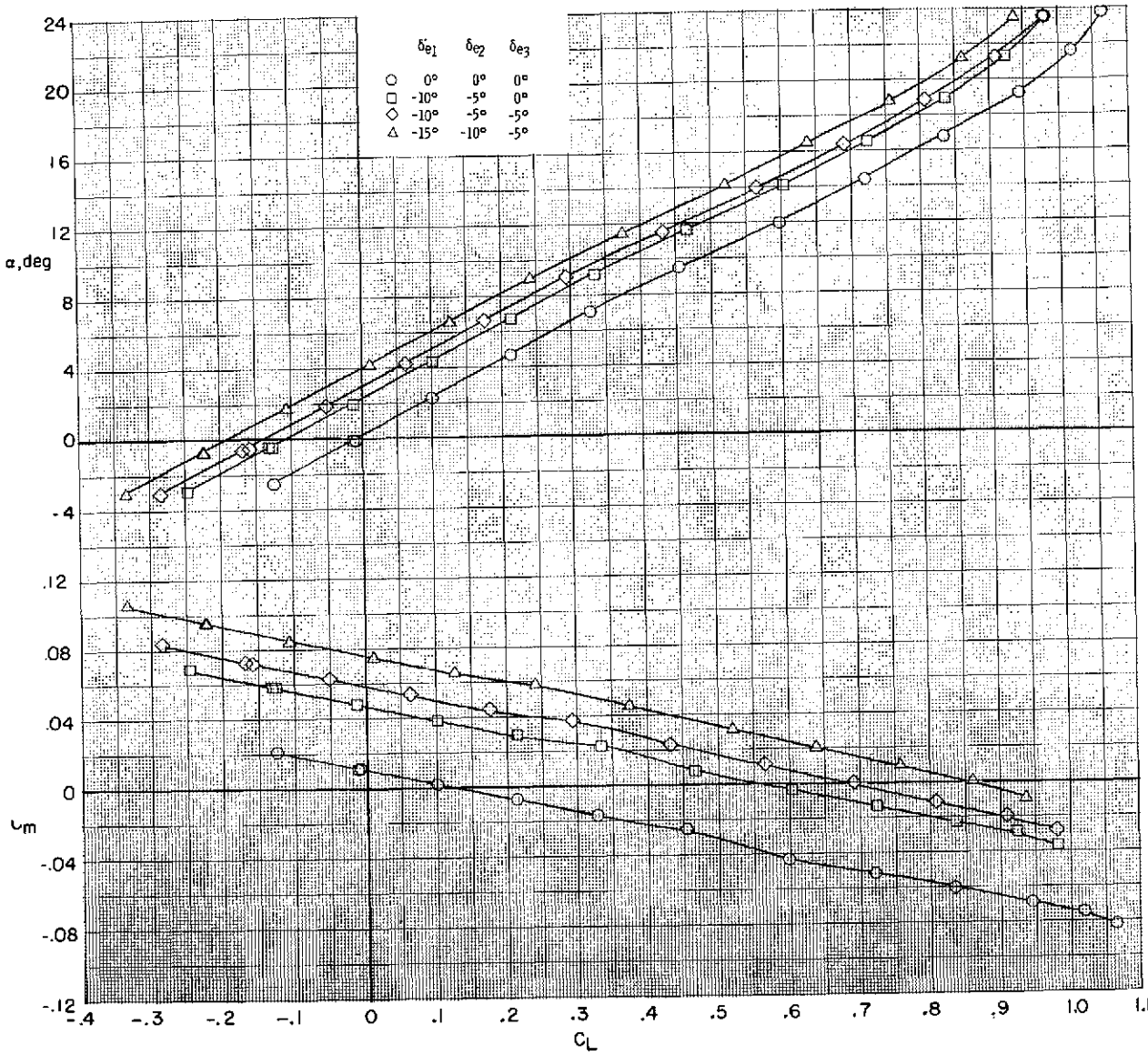

Figure 5.- Effect of elevon deflection on the longitudinal aerodynamic characteristics of BW_TVF_2. $R = 15.8 \times 10^6$.

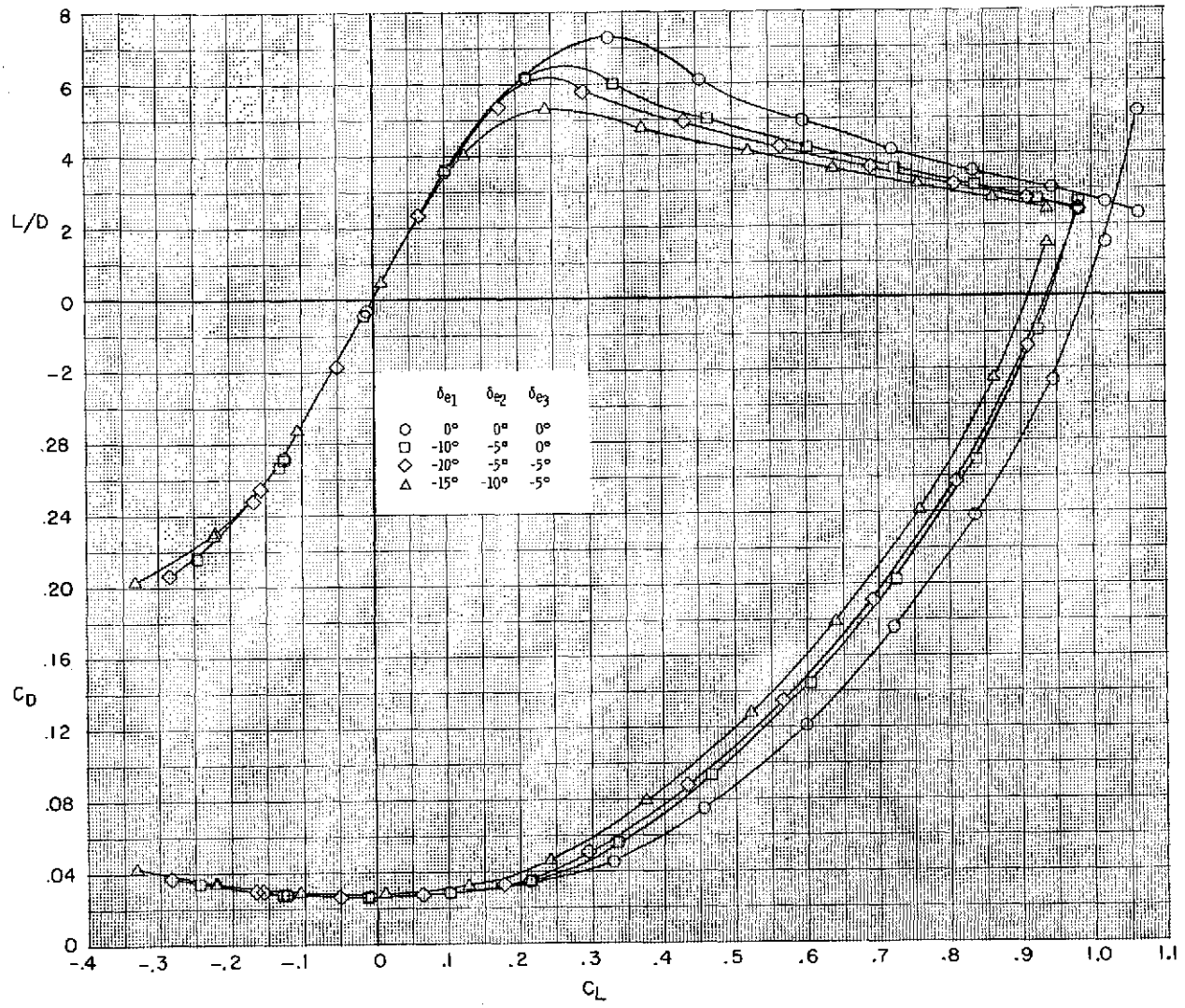

Figure 5.- Concluded.

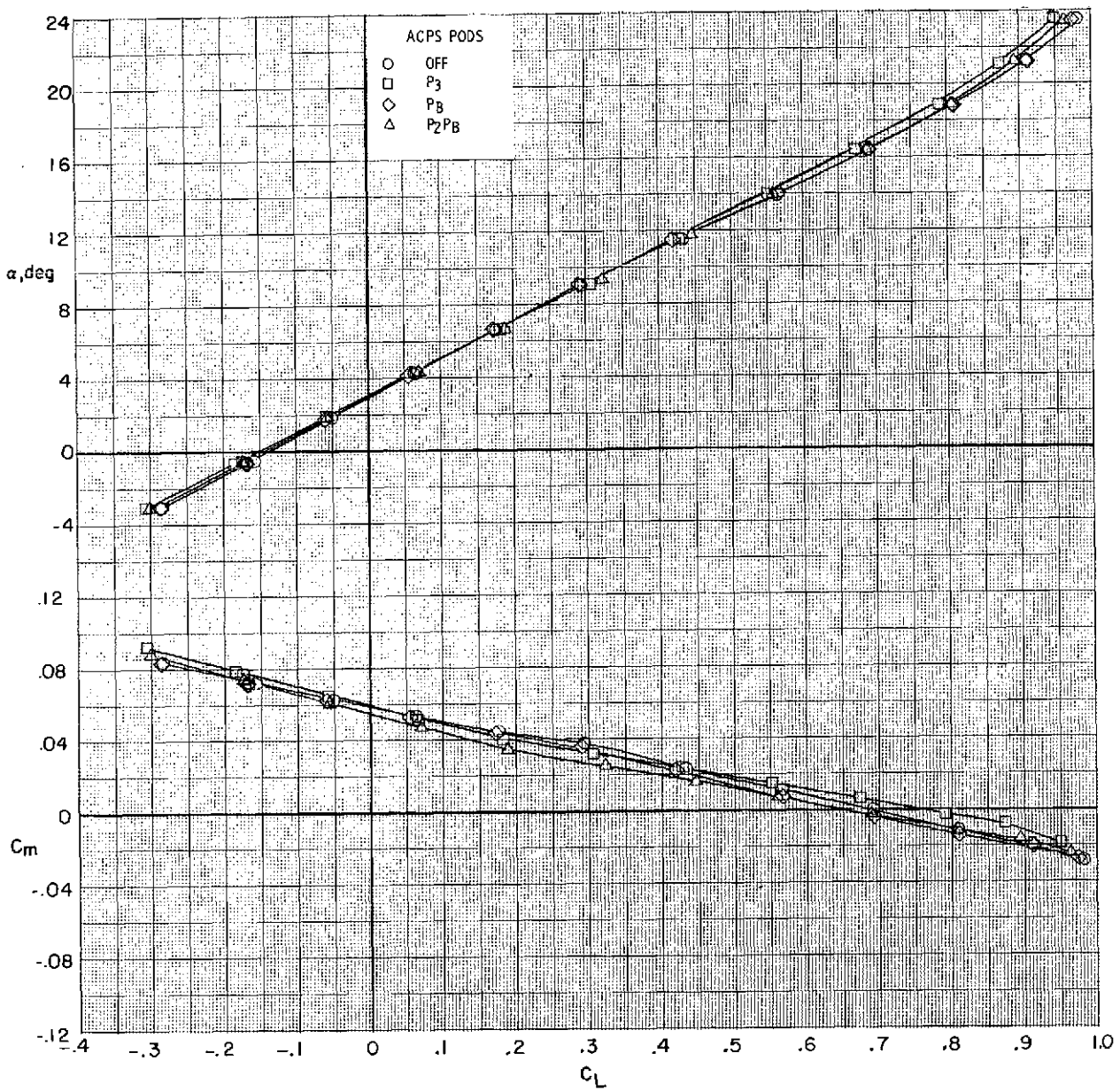

Figure 6.- Effect of wing-tip ACPS pods and body ACPS pods on the longitudinal aerodynamic characteristics of BW_TVF_2. $\delta_{e_1} = -10^o$; $\delta_{e_2} = -5^o$; $\delta_{e_3} = -5^o$; $R = 15.8 \times 10^6$.

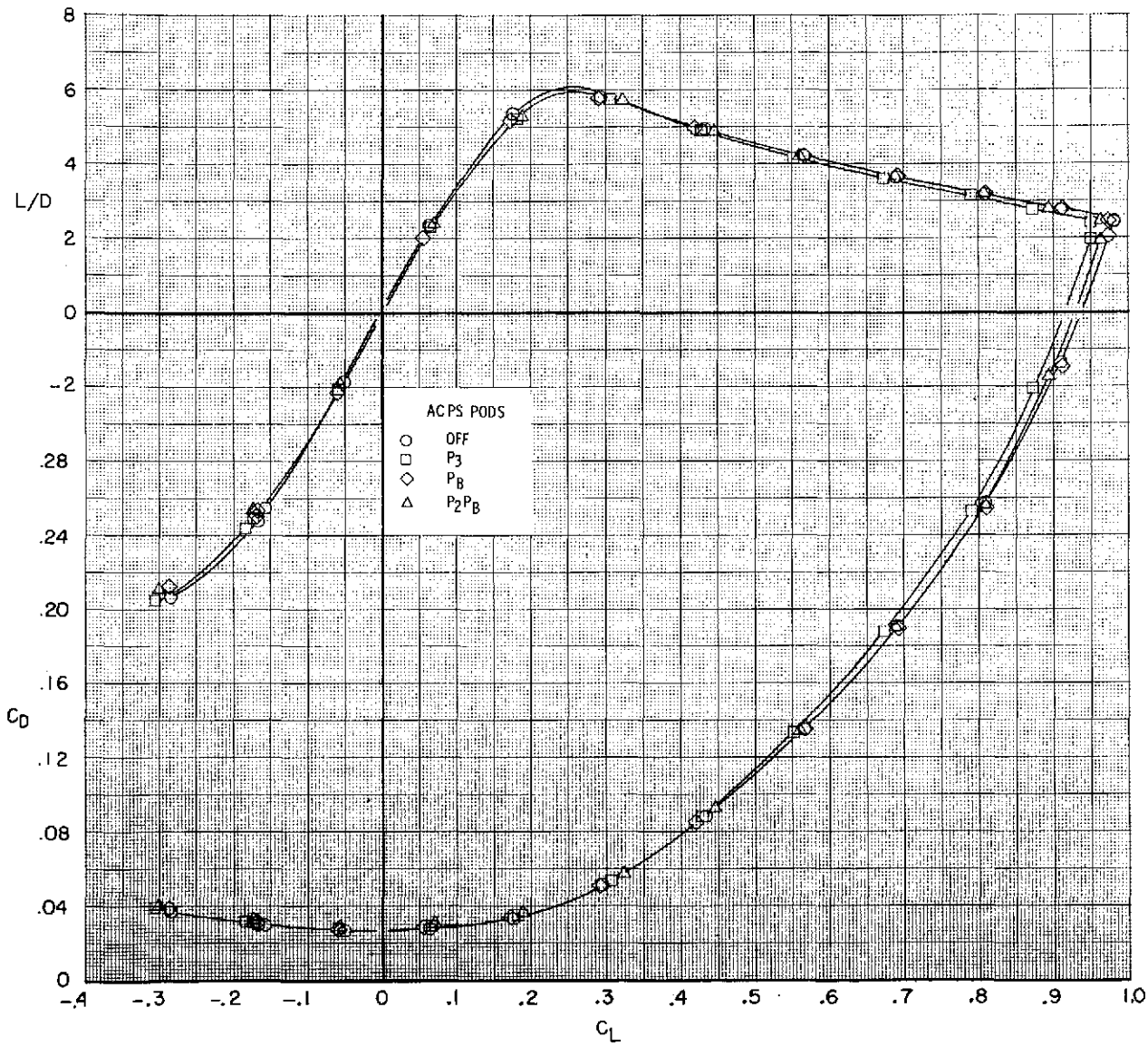

Figure 6.- Concluded.

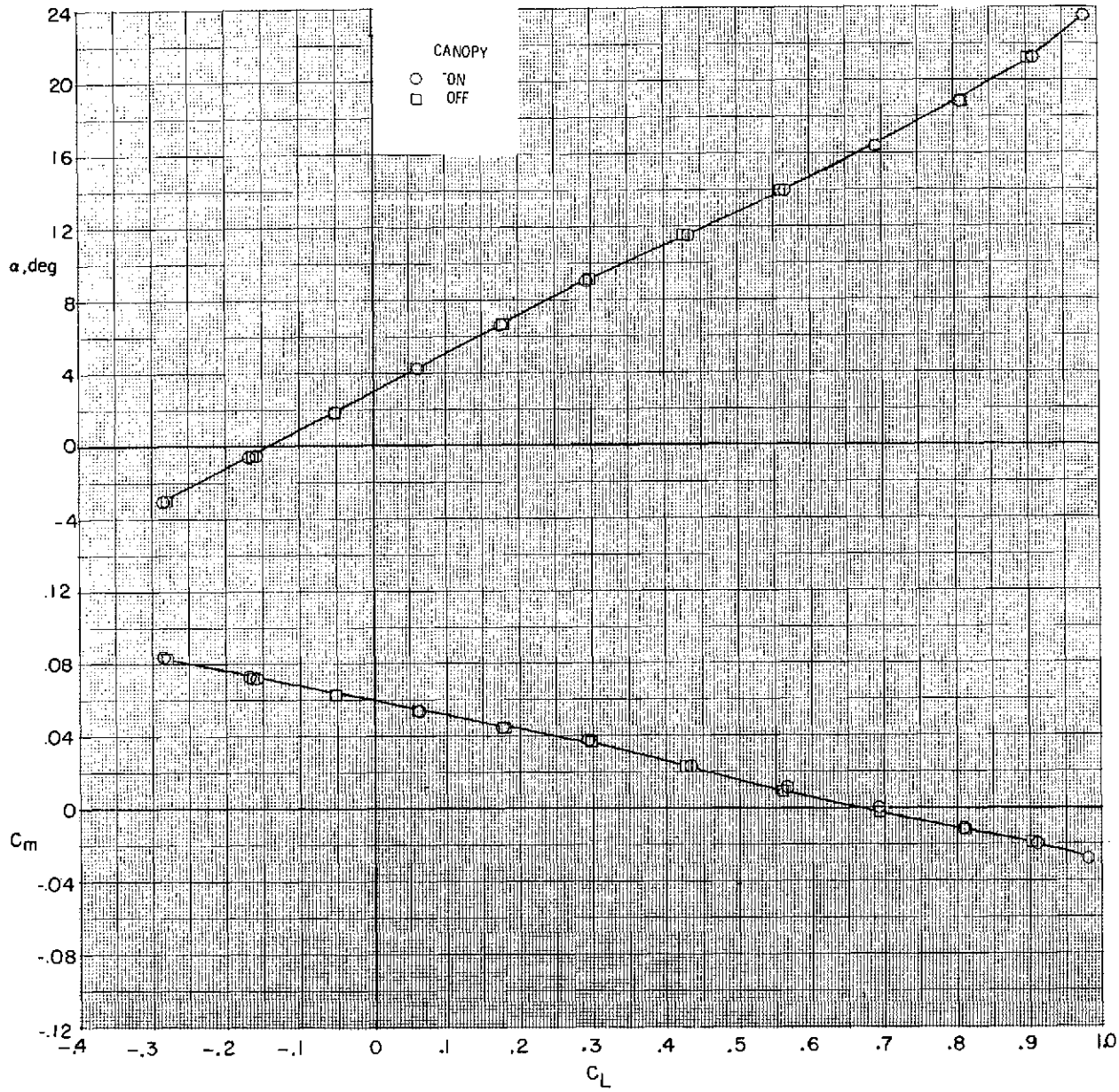

Figure 7.- Effect of canopy on the longitudinal aerodynamic characteristics of BW_TVF_2. $\delta_{e_1} = -10^o$; $\delta_{e_2} = -5^o$; $\delta_{e_3} = -5^o$; $R = 15.8 \times 10^6$.

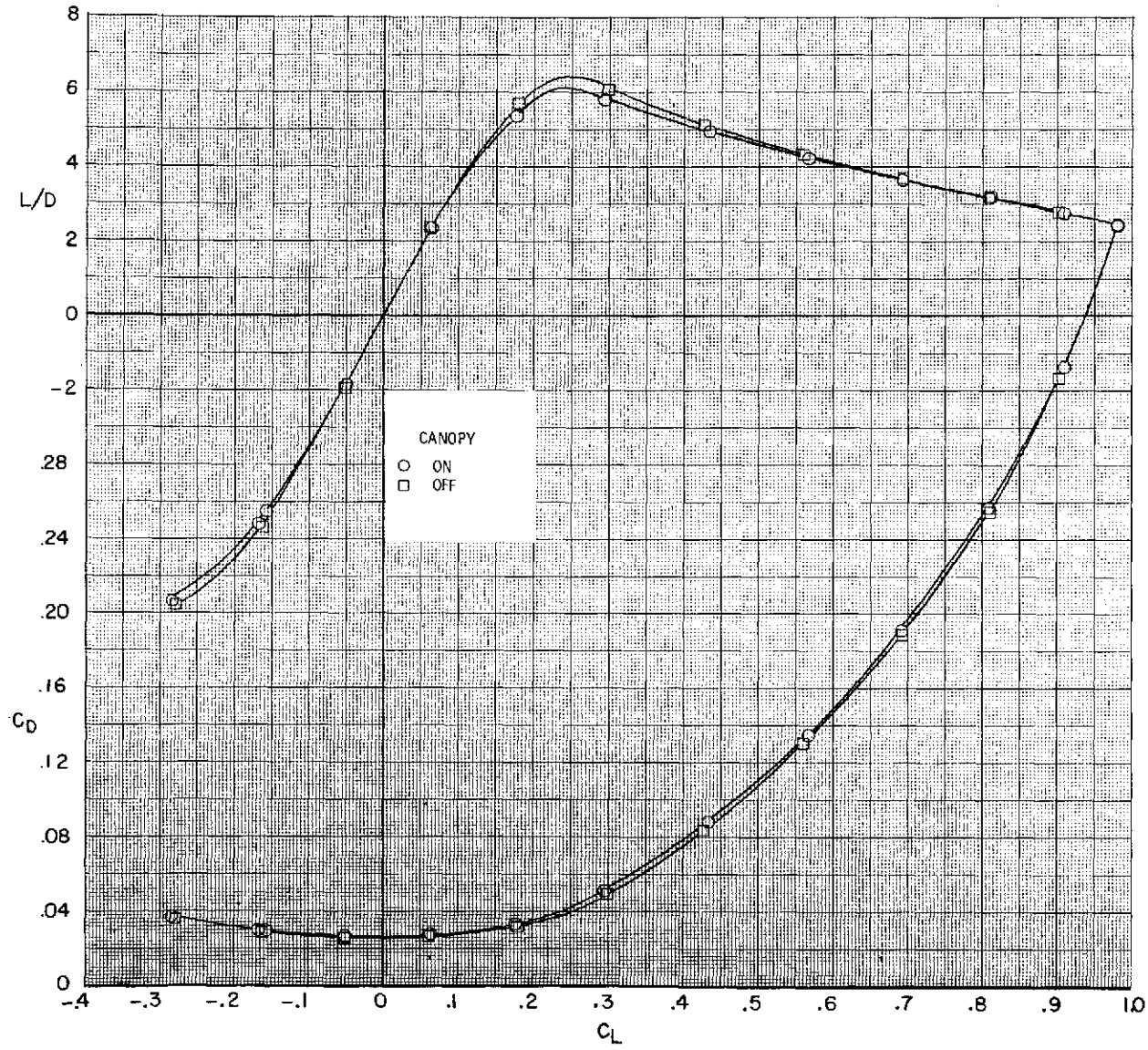

Figure 7.- Concluded.

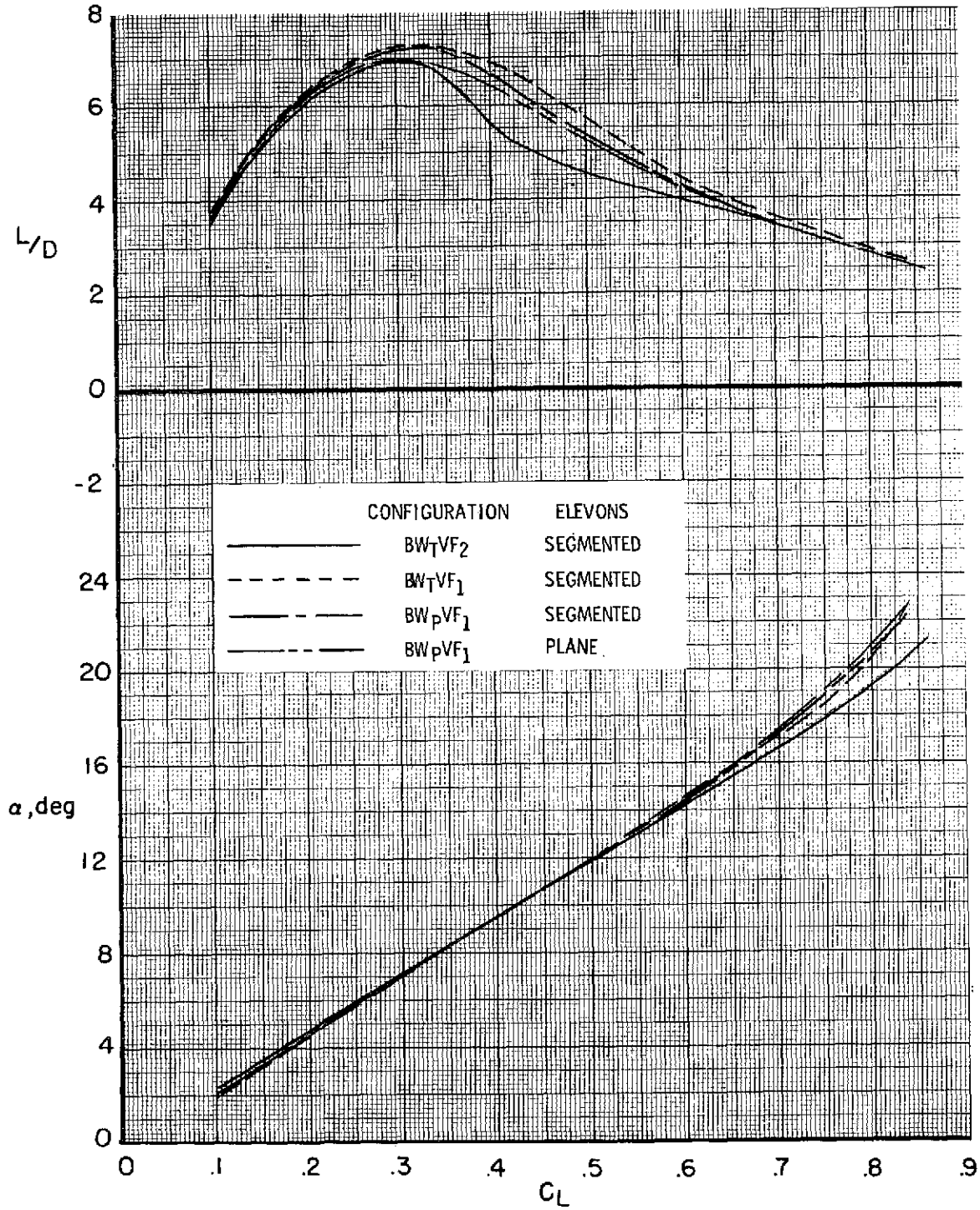

Figure 8.- Trimmed longitudinal aerodynamic characteristics. $R = 15.8 \times 10^6$.

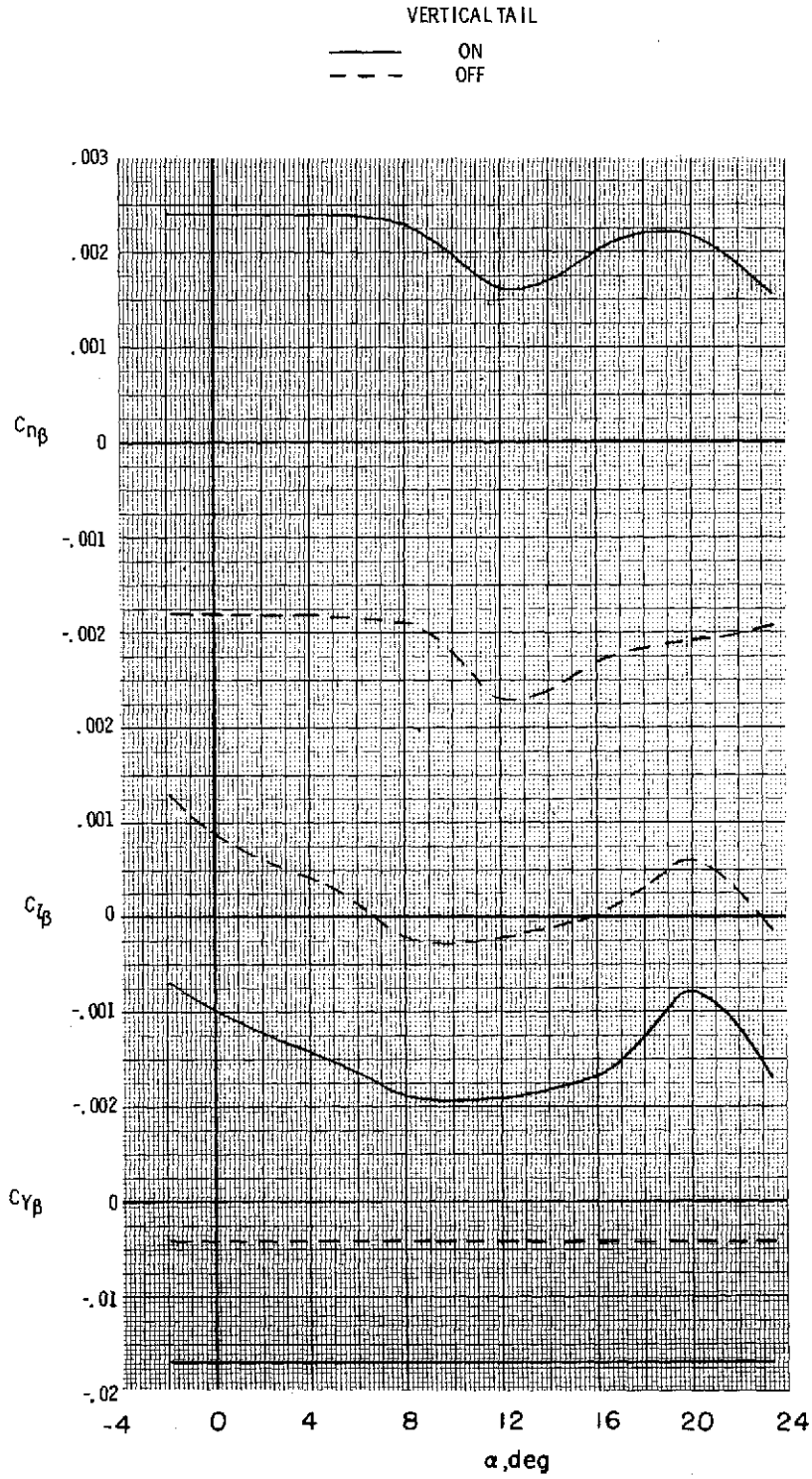

Figure 9.- Lateral directional aerodynamic characteristics of BW_TVF_1 with and without vertical tail. $\delta_{e_1} = -10^o$; $\delta_{e_2} = -5^o$; $\delta_{e_3} = -5^o$; $R = 15.8 \times 10^6$.